3D Fluorescent Hydrogel Origami for Multistage Data Security Protection

Yuchong Zhang, Xiaoxia Le, Yukun Jian, Wei Lu,* Jiawei Zhang, and Tao Chen*

Current fluorescence-based anti-counterfeiting strategies primarily encode information onto single 2D planes and underutilize the possibility of encrypting data inside 3D structures to achieve multistage data security. Herein, a fluorescent-hydrogel-based 3D anti-counterfeiting platform is demonstrated, which extends data encryption capability from single 2D planes to complex 3D hydrogel origami geometries. The materials are based on perylene-tetracarboxylic-acid-functionalized gelatin/poly(vinyl alcohol) hydrogels, which simultaneously show Fe^{3+}-responsive fluorescence quenching, borax-triggered shape memory, and self-healing properties. By employing an origami technique, various complex 3D hydrogel geometries are facilely fabricated. On the basis of these results, a 3D anti-counterfeiting platform is demonstrated, in which the data printed by using Fe^{3+} as the ink are safely protected inside complex 3D hydrogel origami structures. In this way, the encrypted data cannot be read until after specially predesigned procedures (both the shape recovery and UV light illumination actions), indicating higher-level information security than the traditional 2D counterparts. This facile and general strategy opens up the possibility of utilizing 3D fluorescent hydrogel origami for data information encryption and protection.

1. Introduction

Data encryption and protection are of significant importance in military and economic fields, especially for examples in commercial product anti-counterfeit labels.[1,2] One typical chemistry-related example for data security applications is luminescent materials because of their facile design, easy handling, and high-throughput advantages.[2,3] Important documents encrypted by luminescent materials can only be made visible under external light irradiation, leading to increased data

security for their safer transport and communication. However, such fluorescence switching–based single-stage encryption information may be revealed by certain chemical and structural analysis. Therefore, more than one security elements are usually needed for important data in order to increase the difficulty of counterfeiting. A step ahead is the fabrication of more powerful smart luminescent materials (such as multicolor fluorescent materials, persistent room-temperature luminescent materials, and so on),[4,5] which are in favor to realize more efficient multistage data encryption.

Meanwhile, anti-counterfeiting platforms have also evolved from 2D to 3D in order to further enhance information security level.[1] Compared with traditional strategies that primarily code data in single 2D planes, 3D anti-counterfeiting platforms provide many extra advantages. For example, Gao and co-workers have reported a unique type of 3D Janus plasmonic helical nanoaperture to experimentally realize direction-controlled polarization-encrypted data storage with enhanced security for the first time.[6] Ling and co-workers developed a 3D surface-enhanced Raman scattering anti-counterfeiting platform with large encoding capacity, high decoding accuracy, and high flexibility by using a single type of probe molecule.[7] These elegant 3D anti-counterfeiting platforms are capable of providing outputs not in a straightforward predictable manner, and the encrypted information cannot be read until after the specially designed decryption process, making them ideal candidates for multistage information encryption. Nevertheless, fluorescence-based 3D anti-counterfeiting platform, despite being quite promising, has not been demonstrated.
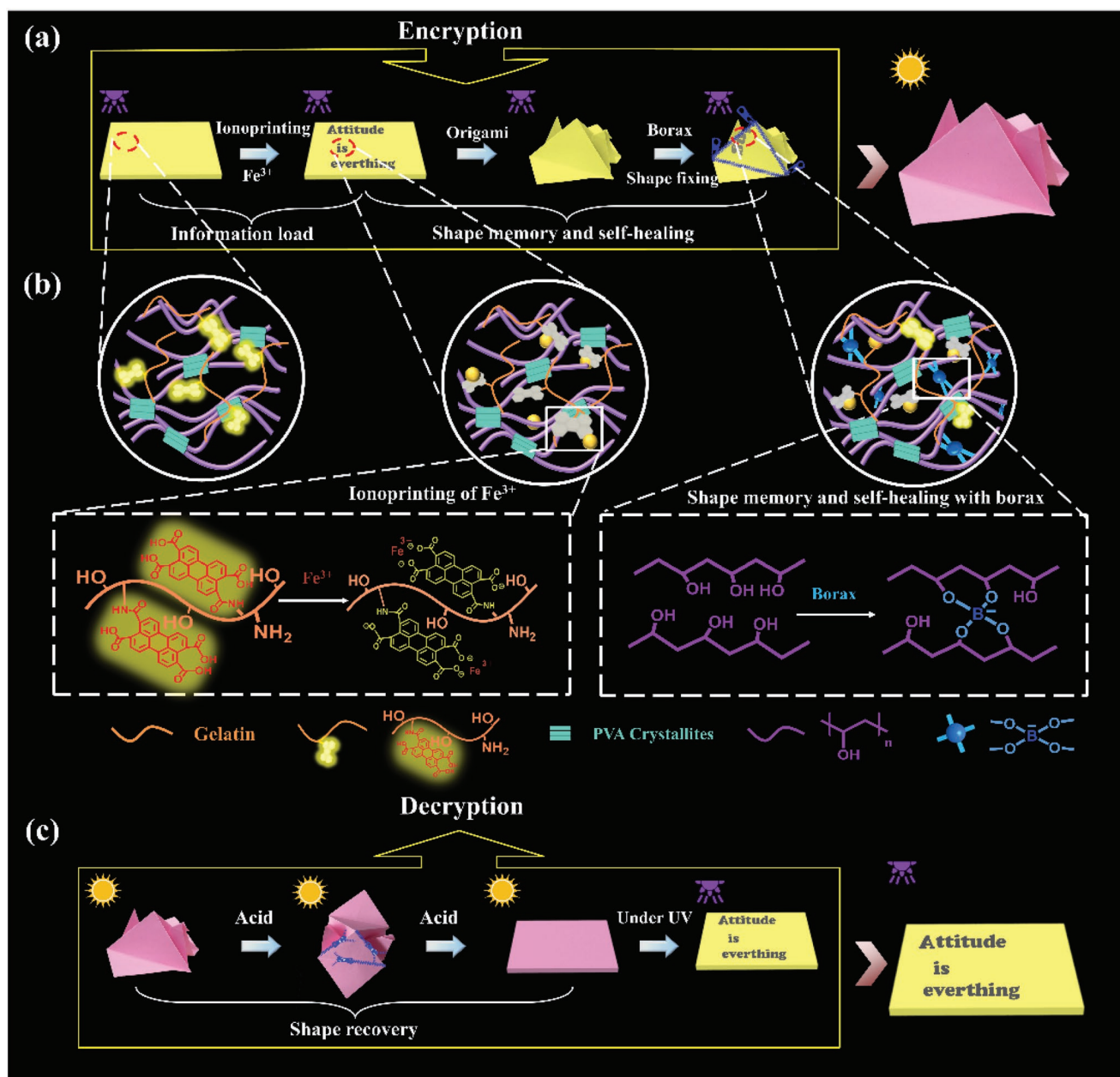
A proof-of-concept material system attempting to demonstrate the fluorescence-based 3D anti-counterfeiting platform is illustrated in **Scheme 1**. The developed system is based on fluorescent hydrogels, because they can be tailored regarding structures, multiple responsiveness, and emission properties.[8] Therefore, there has been a great research interest in developing smart fluorescent hydrogels for encryption applications. For example, Wang and co-workers utilized the ClO^-/SCN^--triggered reversible luminescence response of Tb^{3+}–carboxymethyl cellulose complex hydrogels to realize fingerprint detection and encryption.[9] Zhao et al. reported the employment of structural color poly(*N*-isopropylacrylamide)/reduced graphene oxide hydrogel

Y. Zhang, Dr. X. Le, Y. Jian, Dr. W. Lu, Prof J. Zhang, Prof. T. Chen
Key Laboratory of Marine Materials and Related Technologies
Zhejiang Key Laboratory of Marine Materials and Protective Technologies
Ningbo Institute of Materials Technology and Engineering
Chinese Academy of Sciences
Ningbo 315201, China
E-mail: luwei@nimte.ac.cn; tao.chen@nimte.ac.cn
Y. Zhang, Dr. X. Le, Y. Jian, Prof. T. Chen
University of Chinese Academy of Sciences
19A Yuquan Road, Beijing 100049, China

The ORCID identification number(s) for the author(s) of this article can be found under https://doi.org/10.1002/adfm.201905514.

1905514 (1 of 8)

ADVANCED
SCIENCE NEWS
www.advancedsciencenews.com

ADVANCED
FUNCTIONAL
MATERIALS
www.afm-journal.de

Scheme 1. Schematic illustration showing the data encryption and decryption processes of the developed fluorescent hydrogel–based 3D anti-counterfeiting platform. a,b) The encryption process. Message was first written onto the 2D flat hydrogel films by using Fe^{3+} as the ink, which was then programmed to a 3D crane-shaped hydrogel origami structure by employing origami technique via combined shape memory and self-healing processes. c) The decryption process. The message encrypted in the developed 3D crane-shaped hydrogel origami structure cannot be read until after both the shape recovery and UV light illumination processes.

stripes as dynamic barcode labels for the anti-counterfeiting of different products, which significantly raised the difficulty for counterfeiters to forge.[10] These recent advances open up the possibility of using luminescent hydrogels for data detection, security protection, and information storage. More remarkably, the soft and flexible nature of hydrogel materials enable them to be facilely programmed into various complex 3D geometries by employing such methods as Lego assembly or origami technique.[11,12] Inspired by these impressive advances, we envisioned that 3D origami structures based on multifunctional fluorescent

hydrogels could be used to design robust 3D anti-counterfeiting platform for more effective multistage data encryption.

As shown in Scheme 1a,b, the proof-of-concept fluorescent hydrogels were prepared by repeated freezing/thawing cycles of poly(vinyl alcohol) (PVA) polymer and fluorescent perylene tetracarboxylic acid-grafted gelatin (PTG) polymer solutions. As demonstrated below, the as-prepared hydrogels are endowed with visible Fe^{3+}-controlled fluorescence quenching, suggesting the possibility of writing data onto hydrogel films by using Fe^{3+} as "ink." They also exhibit appealing shape memory and

self-healing capabilities because of the dynamic borate bonds formed between PVA and borax. By employing origami technique, advanced 3D hydrogel origami structures were demonstrated for multistage data encryption. More concretely, data message was first written onto the 2D flat hydrogel films (Scheme 1a), which was then programmed to a desirable 3D hydrogel origami structure via combined shape memory and self-healing processes. Different from paper origami, our 3D hydrogel origami could not be unfolded by external force, because their 3D structures are stabilized and fixed by covalent borate bonds (Scheme 1b). In other words, the protected message cannot be read until after both the shape recovery and UV light illumination processes (Scheme 1c). Notably, the shape recovery conditions are unknown to the public and are only accessible to the authorized party, suggesting greatly enhanced data security of the developed fluorescent hydrogel–based 3D anti-counterfeiting platform. As far as we know, this unique type of hydrogel origami-based 3D anti-counterfeiting platform has never been developed for multistage data encryption, but already shows significantly enhanced security over its traditional 2D counterparts.

2. Results and Discussion

2.1. Fabrication of the Multifunctional Fluorescent PVA–PTG Hydrogels

The fluorescent PTG polymer was prepared and characterized in our previous work.[13] The freezing/thawing process of aqueous PVA–PTG solutions induces physical crosslinks among PVA and PTG chains through a combination of crystalline domains and hydrogen bonds (**Figure 1**a).[14] The PVA crystalline domains act as strong bonds to significantly improve the mechanical strength of the hydrogels. The high-density O-/N-containing groups (e.g., −OH and −NH$_2$) grafted on PTG form vast hydrogen bonds with PVA, making the fluorescent polymer stably and evenly distributed in the hydrogel matrix. It was noticed that the obtained hydrogels emit bright fluorescence over a wide pH range when illuminated under UV light at either 365 nm (Figure 1b,c) or 254 nm (Figure S1a,b, Supporting Information). Interestingly, the emission intensity and color are proved to be typically pH-dependent. Increasing pH value results in growing fluorescence intensity and visible emission color change. This is because the grafted perylene tetracarboxylic acid fluorophores tend to be deprotonated and repel each other in alkaline environment, causing the reduced aggregation–caused emission quenching of perylene fluorophores (Figure 1a).[15]

Shape memory performance of the as-prepared hydrogels was then studied. Due to the strong complexation between adjacent hydroxyl groups of PVA and borax to form covalent boronate ester bonds, the hydrogel films could be quickly programmed to desirable temporary shapes at room temperature after the samples were being deformed by hands and then immersed into borax solution (**Figure 2**a,b). To investigate the influence of freezing–thawing cycles on their shape memory performance, the hydrogel samples with 2–6 freezing–thawing cycles were cut into stripes (30 mm × 3 mm × 1 mm) and

subject to shape memory experiments. The hydrogels prepared after only 1 freezing–thawing cycle was not studied because of its weakness (Figure S2, Supporting Information). As shown in Figure S3 (Supporting Information), the shape fixity ratios (R_f) of these hydrogels are found to decrease gradually from 97% to 66% with increasing freezing–thawing cycles (from 2 to 6) due to higher toughness (Figure 2c,d and Figures S4–S6 (Supporting Information)). But, the shape fixity ratio of tough hydrogels could be remarkably improved by increasing shape memory times (Figure S7, Supporting Information). For the balance of mechanical strength and shape memory properties, the hydrogel samples with 5 freezing–thawing cycles were selected as typical examples and thoroughly investigated.

Note that the swelling ratio of the hydrogels is quite slight in borax solutions within 10 min (Figure S8, Supporting Information) that is enough to complete the shape memory process, indicating that the properties of our hydrogels are almost unaffected by their swelling behaviors. Because of the dynamic nature of covalent borate ester bonds,[14c] these hydrogels could be quickly recovered to the original shapes after being treated in 0.1 M fructose or acid Na$_2$HPO$_4$–citrate buffered solutions (pH = 2) within several minutes (Figures S9 and S10, Supporting Information). Additionally, the tough shape memory hydrogels also exhibit fascinating thermoplasticity owning to their physical crosslinking nature. As shown in Figure 2b, after being cut into pieces and placed in another glass mold at 60 °C, the hydrogels would be softened and merge into such new profiles as five petal flower or fish, suggesting the possibility of arbitrarily changing their permanent shapes as required. Remarkably, the rebuilt hydrogel samples still possess satisfying shape memory performance (Figure S11, Supporting Information).

2.2. Complex 3D Hydrogel Origami Geometries

Other intriguing and important features of the tough shape memory hydrogels include their self-healing properties endowed by dynamic covalent borate ester bonds between PVA and borax. As shown in **Figure 3**a, several pieces of pentagon-shaped hydrogel sheets were first assembled into a lotus-shaped bowl by hands and then treated with borax solutions for a while. During the period, these hydrogel pieces self-healed via borate ester bonds to produce a 3D hydrogel bowl. Note that the self-healed hydrogel pieces also display satisfying mechanical properties and can be stretched by more than 80% of the length (Figure S12, Supporting Information), indicating the freestanding nature and quite good stability of the obtained 3D hydrogel structure. As expected, the fixed 3D hydrogel bowl can be soon recovered into several 2D flat hydrogel pieces in acid solutions. Besides, it is also possible to fabricate 3D hydrogel bowl by starting with one tailored 2D hydrogel piece. Figure 3b illustrates the preparation procedure, in which five petals of the 2D hydrogel piece were first bended by hands and then treated with borax solutions to trigger simultaneous shape memory and self-healing processes. Furthermore, it is possible to construct more complex 3D hydrogel origami structure (e.g., hydrogel dodecahedron demonstrated in Figure 3c) based on synergetic shape memory and self-healing effect. This finding
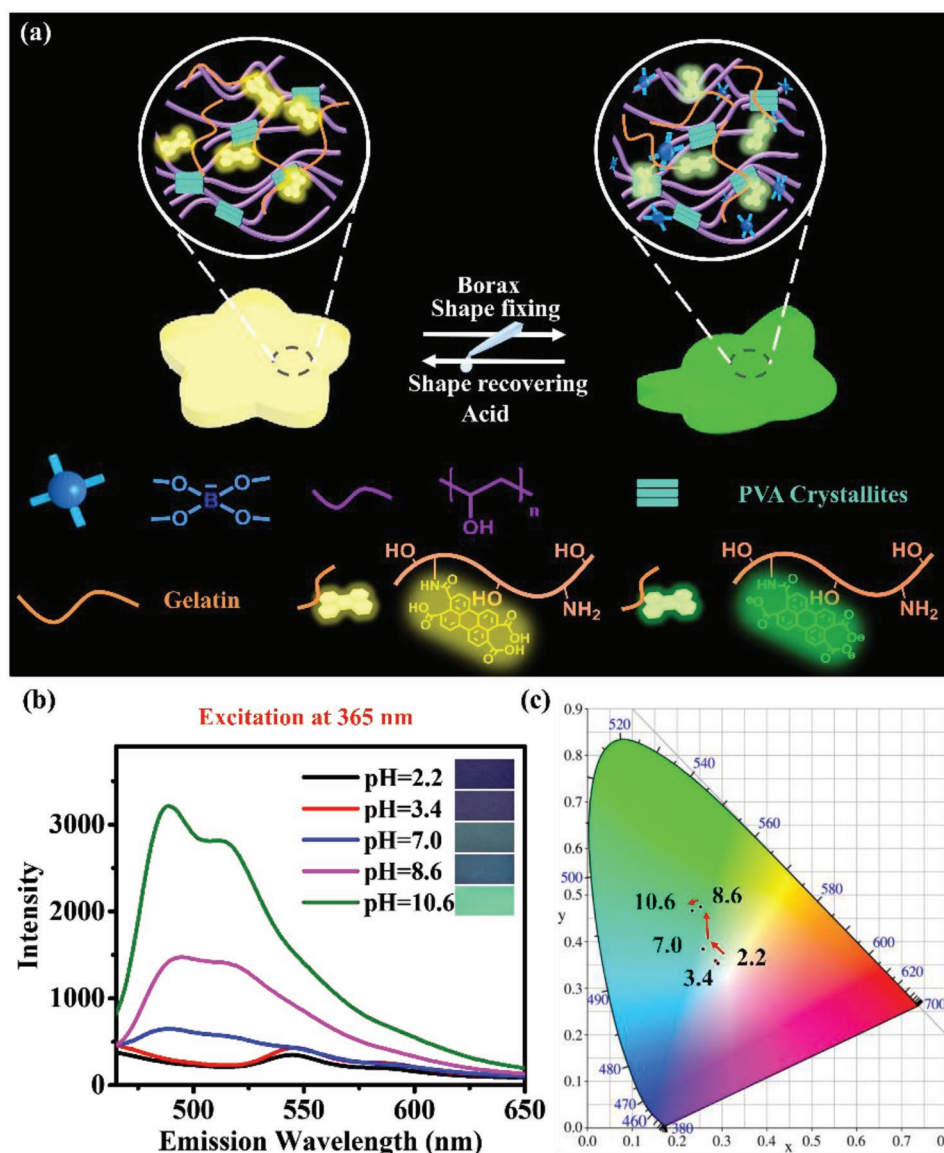
**ADVANCED
SCIENCE NEWS**
www.advancedsciencenews.com

**ADVANCED
FUNCTIONAL
MATERIALS**
www.afm-journal.de

Figure 1. a) Illustration showing the pH-dependent fluorescence response mechanism of PVA–PTG hydrogels. b) Fluorescence spectra of PVA–PTG hydrogels with 5 freezing–thawing cycles, which are treated by various buffered solutions ranging from pH = 2.2 to 10.6 (excitation at 365 nm). Inset shows images of the corresponding hydrogel samples taken under a 365 nm UV light. c) pH-dependent fluorescence color change shown at a standard Commission Internationale de L'Eclairage-1931 color space.

is of interest as it provides an origami-inspired strategy to construct complex 3D structures by starting with the prepared 2D hydrogel samples.

2.3. Fluorescence-Based 3D Anti-Counterfeiting Platform for Multistate Data Encryption

Advanced information encryption and decryption approaches are of significant importance to produce highly efficient anti-counterfeiting identifiers. To this end, the single-stage strategy was first developed based on the fluorescence-switching property of our hydrogels. As shown in **Figure 4**b,c, such information as "SMP" characters and our group logo could be facilely printed

onto the 2D fluorescent hydrogel films by a Fe^{3+}-loaded stamp using the developed ion printing–assisted diffusion–reaction (D–R) method.[12c] Since Fe^{3+} usually serves as a fluorescence quencher to many fluorophores via intramolecular charge transfer mechanism (Figure 4e), high-contrast nonfluorescent patterns were printed onto the "security paper" by Fe^{3+} diffusion from the stamps. More complex information, including 2D quick response (QR) codes, could also be encrypted (Figure 4d). As expected, these encrypted information are not visible with naked eyes or cameras under daylight (Figure 4a). Nevertheless, the written confidential information coded in 2D fluorescent hydrogel films can be directly read by naked eyes or scanned by machines under simple UV light illumination, thus making such fluorescence-based 2D anti-counterfeiting platform less effective.
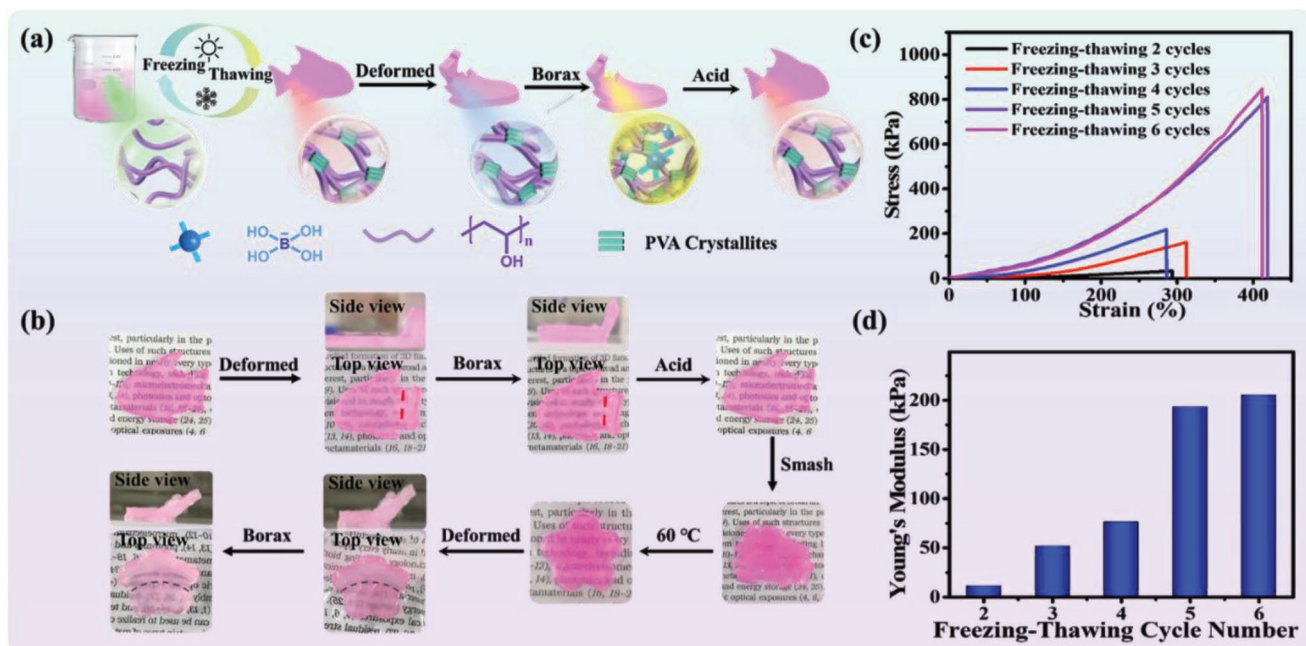
Figure 2. a) Illustration showing the fabrication of the hydrogels through freezing–thawing method and their borax-triggered shape memory mechanism. b) Images showing the shape memory and thermoplastic performance of the hydrogels. c) Tensile stress–strain curves and d) Young's modulus of the hydrogel with different freezing–thawing cycles ranging from 2 to 6.

Besides fluorescence switching property, our hydrogels were also demonstrated to bear satisfying mechanically tough, thermoplastic, self-healing, and shape memory features, which encourage us to capitalize on these advantages synergetically to produce more efficient anti-counterfeit identifiers. As

demonstrated in Figure S13a (Supporting Information), two hydrogel pieces were put together and printed with the "IP" word using the abovementioned ion printing–assisted D–R method. After the top one stretched by hands and fixed in borax solutions to memorize the elongated temporary shape, a
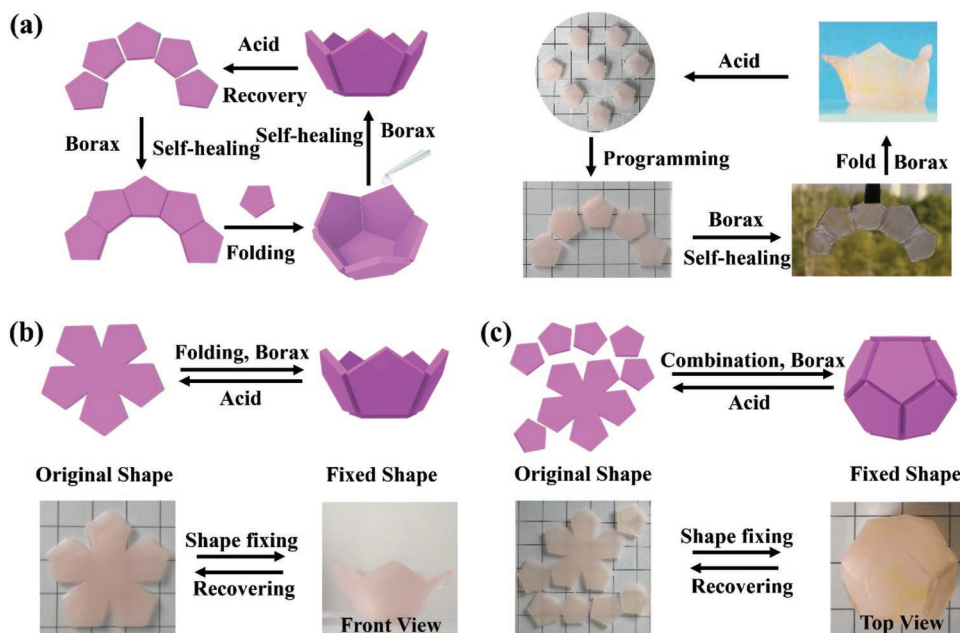

Figure 3. Complex 3D hydrogel origami geometries. a) Six pieces of regular pentagon-shaped PVA–PTG hydrogel sheets were brought together and self-healed in the presence of borax solution to form a freestanding 3D hydrogel bowl. b) Fabrication of a freestanding 3D hydrogel bowl by starting with one tailored 2D hydrogel piece via the combination of shape memory and self-healing abilities. c) Fabrication of more complex 3D hydrogel dodecahedron by starting with several 2D hydrogel pieces via the combination of shape memory and self-healing abilities.
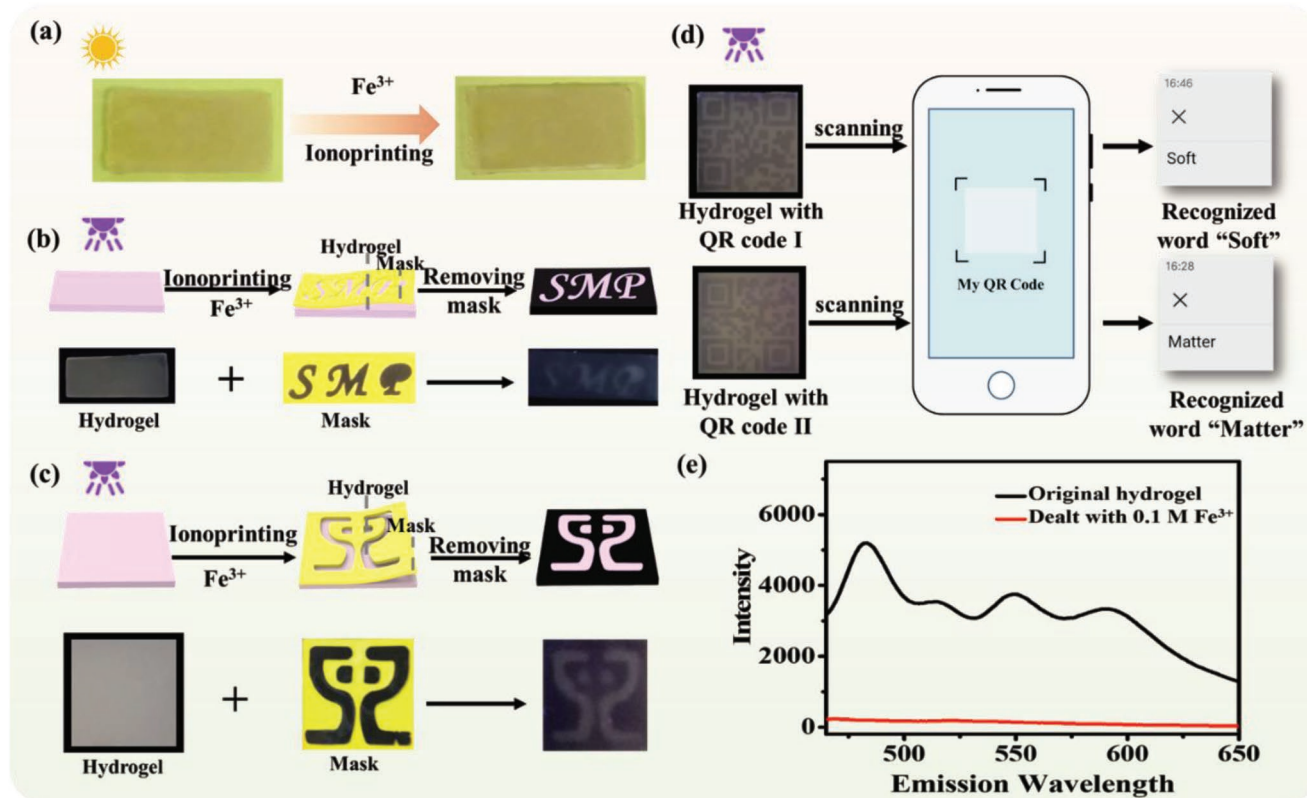
Figure 4. Fluorescence-based 2D anti-counterfeiting platform. a) Images of the hydrogel films before and after ionoprinting by using Fe^{3+} as ink. Illustration and images of the hydrogel films printed with b) "SMP" characters, c) our group logo, and d) QR codes representing "Soft" and "Matter" by Fe^{3+}-loaded stamps. e) Fluorescence spectra of the hydrogel films before and after being treated by Fe^{3+} solutions (0.1 M).

new-type 2D anti-counterfeiting identifier was developed via a collective action of shape memory and fluorescence switching properties. The protected information can only be decrypted under UV light illumination after the acid-triggered shape recovery of the top hydrogel piece. Either UV light illumination or acid treatment leads to no or wrong information. What is more, it has been further demonstrated to code information in three dimensions using similar strategy. For example, the 2D hydrogel films with printed binary data "01010000" that represents "P" was programmed to temporary spiral shape to produce 3D anti-counterfeiting identifier (Figure S13b, Supporting Information).

To enhance encoding complexity, more promising 3D anti-counterfeiting platforms were fabricated on the basis of complex 3D hydrogel origami structures via the collective self-healing, shape memory, and fluorescence switching actions. As shown in **Figure 5**a, one 2D hydrogel film printed with "UCAS" letters was first folded into a 3D tetrahedron shape by hands and then immersed into borax solutions for a few seconds. During this period, the 3D tetrahedron-shaped hydrogel origami structure was fixed by dynamic covalent borate ester bonds between PVA and borax. In this way, the "UCAS" data were successfully encoded inside the 3D hydrogel geometry. In a similar vein, the "Q1A2Z3" data were encrypted inside a 3D cube-shaped hydrogel origami structure (Figure 5b). Obviously, these encrypted data could not be observed under either UV or visible light illumination. To decrypt the data, an additional

acid-triggered shape recovery process must be conducted (Figure 5a-I,II). If these hydrogel origami geometries were not unfolded by the specially designed steps, for example, dismantling them with external force, incorrect information would be presented (Figure 5b-III). Furthermore, more complex 3D crane-shaped hydrogel origami was developed by starting with a square-shaped 2D hydrogel film to conceal the message "Attitude is everything" (Figure 5c). Since the shape recovery conditions (in Na_2HPO_4–citrate buffer solution (pH = 2.2) for several minutes) are usually unknown to the public, more superior data security level was realized in these 3D anti-counterfeiting platforms than their traditional 2D counterparts. In view of the modular design principle of the developed 3D anti-counterfeiting platforms, the proposed strategy could be generally applicable to the multistage protection of many other data (Figure S14a–c, Supporting Information).

3. Conclusion

In summary, we have demonstrated an advanced fluorescence-based 3D anti-counterfeiting platform, where data information is encrypted in 3D hydrogel origami geometries. The materials are based on perylene tetracarboxylic acid-functionalized gelatin/PVA hydrogels, which are endowed with satisfying mechanical strength and Fe^{3+}-controlled fluorescence quenching, as well as borax-triggered shape memory and
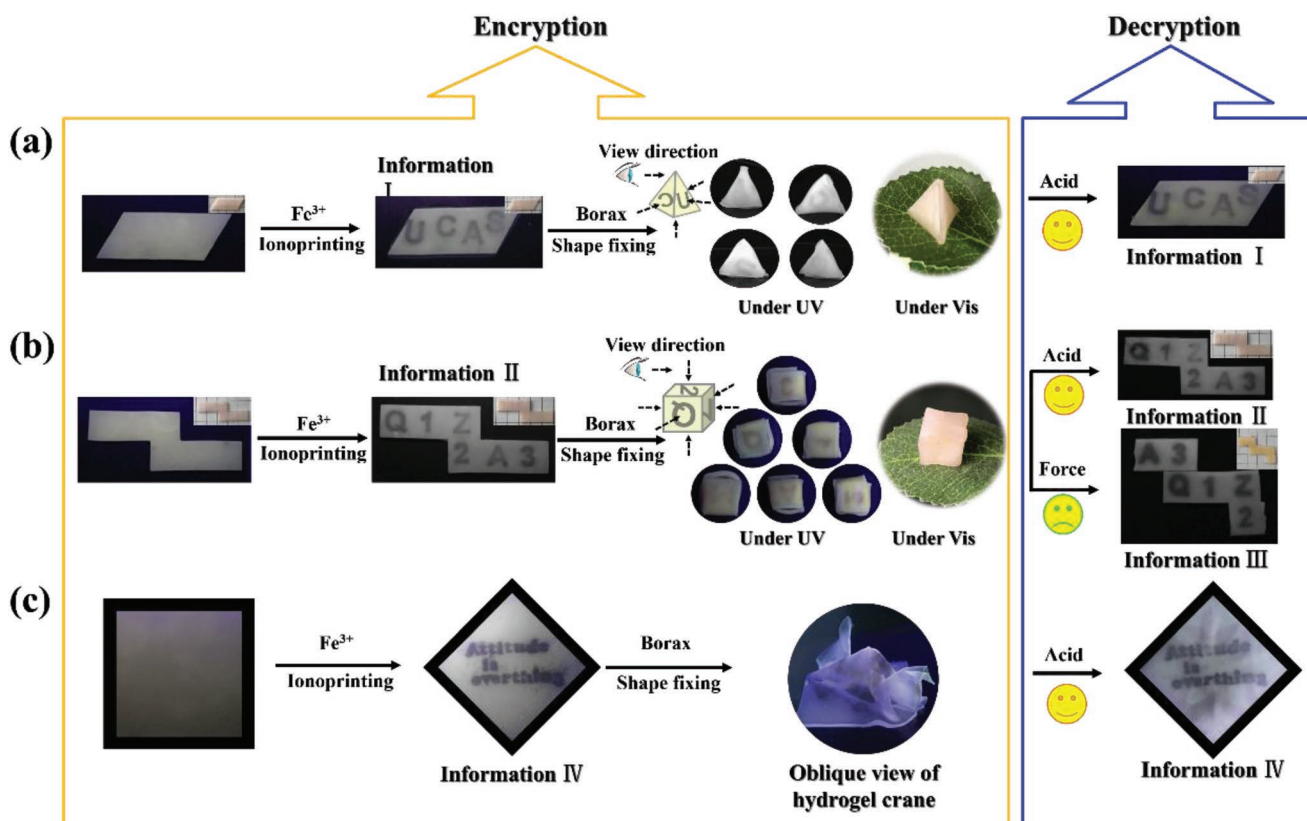
Figure 5. Fluorescence-based 3D anti-counterfeiting platform. 2D hydrogel films printed with a) "UCAS," b) "Q1A2Z3," c) "Attitude is everything" messages were first folded into 3D tetrahedron, cube, and crane shapes by hands, respectively, and then immersed into borax solutions for a while (10 s – 3 min). During this period, these 3D hydrogel origami structures were fixed by dynamic covalent borate ester bonds between PVA and borax. In this way, these data were successfully encoded inside the 3D hydrogel geometries.

self-healing properties. Based on synergetic effect of these appealing properties, various complex 3D hydrogel origami geometries have been constructed, which could be used to protect data information in three dimensions. Information encrypted in these 3D hydrogel origami structures can only be decrypted after specially predesigned procedures (e.g., under UV illumination after treating these 3D hydrogel structures in acid solutions for shape recovery). Notably, the specially predesigned procedures are unknown to the public and are only accessible to the authorized party, suggesting the superior encryption security of our 3D platform to its traditional 2D counterparts. This facile and general strategy opens up the possibility of utilizing 3D fluorescent hydrogel origami for data information encryption and protection.

Supporting Information

Supporting Information is available from the Wiley Online Library or from the author.

Acknowledgements

Conflict of Interest

The authors declare no conflict of interest.

Keywords

[1] G. C. Phan-Quang, X. Han, C. S. L. Koh, H. Y. F. Sim, C. L. Lay, S. X. Leong, Y. H. Lee, N. Pazos-Perez, R. A. Alvarez-Puebla, X. Y. Ling, *Acc. Chem. Res.* **2019**, *52*, 1844.

[2] L. Gu, H. Shi, L. Bian, M. Gu, K. Ling, X. Wang, H. Ma, S. Cai, W. Ning, L. Fu, H. Wang, S. Wang, Y. Gao, W. Yao, F. Huo, Y. Tao, Z. An, X. Liu, W. Huang, *Nat. Photonics* **2019**, *13*, 406.

[3] a) O. Guillou, C. Daiguebonne, G. Calvez, K. Bernot, *Acc. Chem. Res.* **2016**, *49*, 844; b) X. Qin, J. Xu, Y. Wu, X. Liu, *ACS Cent. Sci.* **2019**, *5*, 29; c) J. Andreasson, U. Pischel, *Chem. Soc. Rev.* **2018**, *47*, 2266.

[4] a) P. Long, Y. Feng, C. Cao, Y. Li, J. Han, S. Li, C. Peng, Z. Li, W. Feng, *Adv. Funct. Mater.* **2018**, *28*, 1800791; b) W. Tian, J. Zhang, J. Yu, J. Wu, J. Zhang, J. He, F. Wang, *Adv. Funct. Mater.* **2018**, *28*, 1703548; c) M. Tu, H. Reinsch, S. Rodriguez-Hermida, R. Verbeke, T. Stassin, W. Egger, M. Dickmann, B. Dieu, J. Hofkens, I. Vankelecom, N. Stock, R. Ameloot, *Angew. Chem., Int. Ed.* **2019**, *58*, 2423; d) H. Yang, Y. Liu, Z. Guo, B. Lei, J. Zhuang, X. Zhang, Z. Liu, C. Hu, *Nat. Commun.* **2019**, *10*, 1789; e) M. R. Carro-Temboury, R. Arppe, T. Vosch, T. J. Sorensen, *Sci. Adv.* **2018**, *4*, e1701384; f) Y. Su, S. Z. F. Phua, Y. B. Li, X. J. Zhou, D. Jana, G. F. Liu, W. Q. Lim, W. K. Ong, C. L. Yang, Y. L. Zhao, *Sci. Adv.* **2018**, *4*, eaas9732.

[5] a) D. Tian, Z. Zhu, L. Xu, H. Cong, J. Zhu, *Mater. Horiz.* **2019**, *6*, 1215; b) H. Sun, S. Liu, W. Lin, K. Y. Zhang, W. Lv, X. Huang, F. Huo, H. Yang, G. Jenkins, Q. Zhao, W. Huang, *Nat. Commun.* **2014**, *5*, 3601; c) J. Wang, X. Gu, H. Ma, Q. Peng, X. Huang, X. Zheng, S. H. P. Sung, G. Shan, J. W. Y. Lam, Z. Shuai, B. Z. Tang, *Nat. Commun.* **2018**, *9*, 2963; d) W. Zhao, T. S. Cheung, N. Jiang, W. Huang, J. W. Y. Lam, X. Zhang, Z. He, B. Z. Tang, *Nat. Commun.* **2019**, *10*, 1595.

[6] Y. Chen, X. Yang, J. Gao, *Light: Sci. Appl.* **2019**, *8*, 45.

[7] Y. Liu, Y. H. Lee, M. R. Lee, Y. Yang, X. Y. Ling, *ACS Photonics* **2017**, *4*, 2529.

[8] a) L. Chen, Y.-A. Yin, Y.-X. Liu, L. Lin, M.-J. Liu, *Chin. J. Polym. Sci.* **2017**, *35*, 1181; b) X. Li, M. J. Serpe, *Adv. Funct. Mater.* **2016**, *26*, 3282; c) C. Ma, W. Lu, X. Yang, J. He, X. Le, L. Wang, J. Zhang, M. J. Serpe, Y. Huang, T. Chen, *Adv. Funct. Mater.* **2018**, *28*, 1704568; d) X. Le, W. Lu, J. Zhang, T. Chen, *Adv. Sci.* **2019**, *6*, 1801584; e) W. Lu, X. Le, J. Zhang, Y. Huang, T. Chen, *Chem. Soc. Rev.* **2017**, *46*, 1284; f) S. J. Jeon, A. W. Hauser, R. C. Hayward, *Acc. Chem. Res.* **2017**, *50*, 161; g) C. Lowenberg, M. Balk, C. Wischke, M. Behl, A. Lendlein, *Acc. Chem. Res.* **2017**, *50*, 723; h) H. Yuk, B. Lu, X. Zhao, *Chem. Soc. Rev.* **2019**, *48*, 1642; i) T. Matsuda, R. Kawakami, R. Namba, T. Nakajima, J. P. Gong, *Science* **2019**, *363*, 504; j) R. Kempaiah, Z. Nie, *J. Mater. Chem. B* **2014**, *2*, 2357; k) J. Shang, P. Theato, *Soft Matter* **2018**, *14*, 8401.

[9] J. Hai, T. Li, J. Su, W. Liu, Y. Ju, B. Wang, Y. Hou, *Angew. Chem., Int. Ed.* **2018**, *57*, 6786.

[10] Z. Zhao, H. Wang, L. Shang, Y. Yu, F. Fu, Y. Zhao, Z. Gu, *Adv. Mater.* **2017**, *29*, 1704569.

[11] a) Y. Zhang, J. Liao, T. Wang, W. Sun, Z. Tong, *Adv. Funct. Mater.* **2018**, *28*, 1707245; b) E. Zhang, T. Wang, W. Hong, W. Sun, X. Liu, Z. Tong, *J. Mater. Chem. A* **2014**, *2*, 15633; c) L. Huang, R. Jiang, J. Wu, J. Song, H. Bai, B. Li, Q. Zhao, T. Xie, *Adv. Mater.* **2017**, *29*, 1605390; d) C. Ma, T. Li, Q. Zhao, X. Yang, J. Wu, Y. Luo, T. Xie, *Adv. Mater.* **2014**, *26*, 5665; e) Q. Zhao, X. Yang, C. Ma, D. Chen, H. Bai, T. Li, W. Yang, T. Xie, *Mater. Horiz.* **2016**, *3*, 422.

[12] a) Z. Zhao, S. Zhuo, R. Fang, L. Zhang, X. Zhou, Y. Xu, J. Zhang, Z. Dong, L. Jiang, M. Liu, *Adv. Mater.* **2018**, *30*, 1804435; b) M. J. Liu, Y. Ishida, Y. Ebina, T. Sasaki, T. Hikima, M. Takata, T. Aida, *Nature* **2015**, *517*, 68; c) X. Peng, T. Liu, Q. Zhang, C. Shang, Q.-W. Bai, H. Wang, *Adv. Funct. Mater.* **2017**, *27*, 1701962; d) Y. Zhou, A. W. Hauser, N. P. Bende, M. G. Kuzyk, R. C. Hayward, *Adv. Funct. Mater.* **2016**, *26*, 5447; e) L. Liu, A. Ghaemi, S. Gekle, S. Agarwal, *Adv. Mater.* **2016**, *28*, 9792; f) K. Sano, Y. Ishida, T. Aida, *Angew. Chem., Int. Ed.* **2018**, *57*, 2532; g) T. Chen, H. Li, Z. Li, Q. Jin, J. Ji, *Mater. Horiz.* **2016**, *3*, 581; h) W. X. Fan, C. Y. Shan, H. Y. Guo, J. W. Sang, R. Wang, R. R. Zheng, K. Y. Sui, Z. H. Nie, *Sci. Adv.* **2019**, *5*, eaav7174; i) X. Ji, B. Shi, H. Wang, D. Xia, K. Jie, Z. L. Wu, F. Huang, *Adv. Mater.* **2015**, *27*, 8062; j) Z. J. Wang, W. Hong, Z. L. Wu, Q. Zheng, *Angew. Chem., Int. Ed.* **2017**, *56*, 15974; k) Z. J. Wang, C. N. Zhu, W. Hong, Z. L. Wu, Q. Zheng, *Sci. Adv.* **2017**, *3*, e1700348.

[13] B. Y. Wu, X. X. Le, Y. K. Jian, W. Lu, Z. Y. Yang, Z. K. Zheng, P. Theato, J. W. Zhang, A. Zhang, T. Chen, *Macromol. Rapid Commun.* **2019**, *40*, 1800648.

[14] a) Q. Rong, W. Lei, L. Chen, Y. Yin, J. Zhou, M. Liu, *Angew. Chem., Int. Ed.* **2017**, *56*, 14159; b) S. Huang, F. Wan, S. Bi, J. Zhu, Z. Niu, J. Chen, *Angew. Chem., Int. Ed.* **2019**, *58*, 4313; c) Y. C. Zhang, X. X. Le, W. Lu, Y. K. Jian, J. W. Zhang, T. Chen, *Macromol. Mater. Eng.* **2018**, *303*, 1800144; d) H. Zhang, H. Xia, Y. Zhao, *ACS Macro Lett.* **2012**, *1*, 1233; e) Y. X. Li, X. Fang, Y. Wang, B. H. Ma, J. Q. Sun, *Chem. Mater.* **2016**, *28*, 6975; f) Y. Li, L. Liang, C. Liu, Y. Li, W. Xing, J. Sun, *Adv. Mater.* **2018**, *30*, 1707146.

[15] W. Tian, J. Zhang, J. Yu, J. Wu, H. Nawaz, J. Zhang, J. He, F. Wang, *Adv. Opt. Mater.* **2016**, *4*, 2044.